Supporting information

Embedding AIE-featured $Ag_{28}Au_1$ nanoclusters with ZIF-8 for improved photodynamic wound healing through bacterial eradication

Qiuxia He,[a] Zhen Jiang,[a] Hongli Jiang,[c] Songjie Han,[a] Guoping Yang,[b] Xun Yuan*[a] and Haiguang Zhu*[a]*

[a]College of Materials Science and Engineering, Qingdao University of Science and Technology (QUST), 53 Zhengzhou Rd., Shibei District, Qingdao 266042, P. R. China. Email address: yuanxun@qust.edu.cn (Xun Yuan), zhuhg@qust.edu.cn (Haiguang Zhu).

[b]School of Chemistry, Biology and Material Science, Jiangxi Province Key Laboratory of Synthetic Chemistry, Jiangxi Key Laboratory for Mass Spectrometry and Instrumentation, East China

[c]University of Technology, Nanchang 330013, China. Department of Respiratory and Critical Care Medicine, Qingdao Eighth People's Hospital, Qingdao 266121, China.

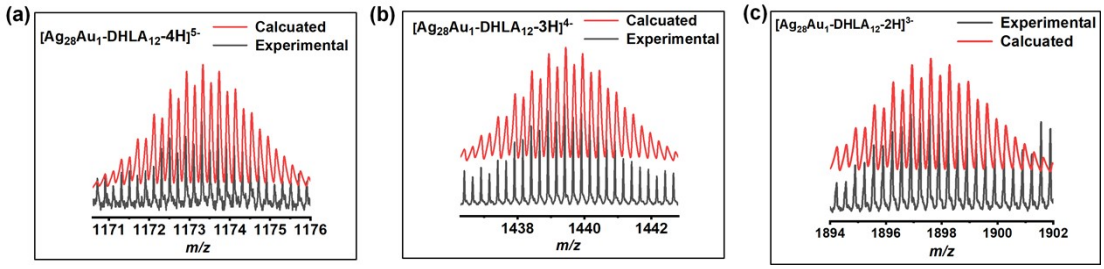

Figure S1. Isotope patterns of (a) $[Ag_{28}Au_1(DHLA)_{12}\text{-}4H]^{5-}$, (b) $[Ag_{28}Au_1(DHLA)_{12}\text{-}3H]^{4-}$, and (c) $[Ag_{28}Au_1(DHLA)_{12}\text{-}2H]^{3-}$ species acquired experimentally (black curve) and theoretically (red curve).

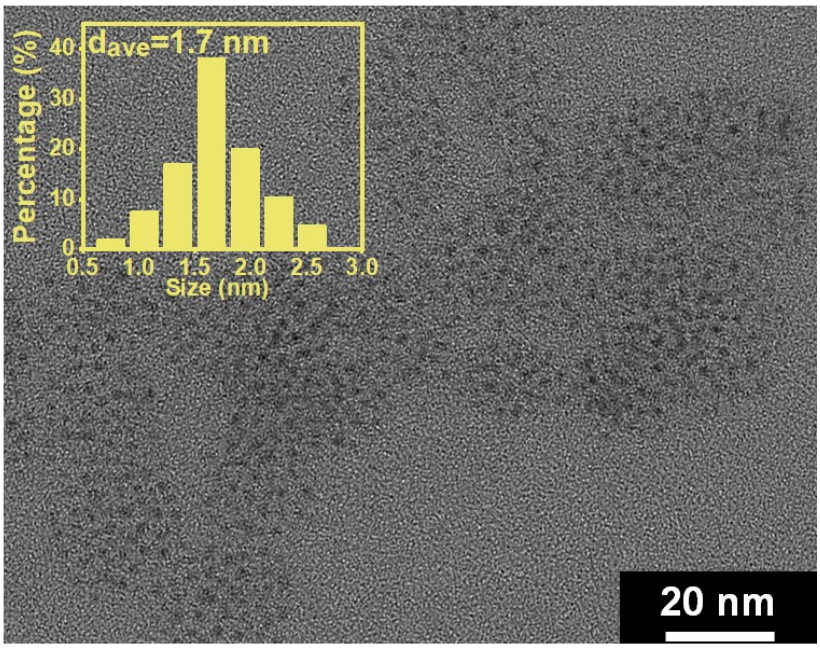

Figure S2. TEM image and size distribution histogram (inset) of the $Ag_{28}Au_1$ NCs.

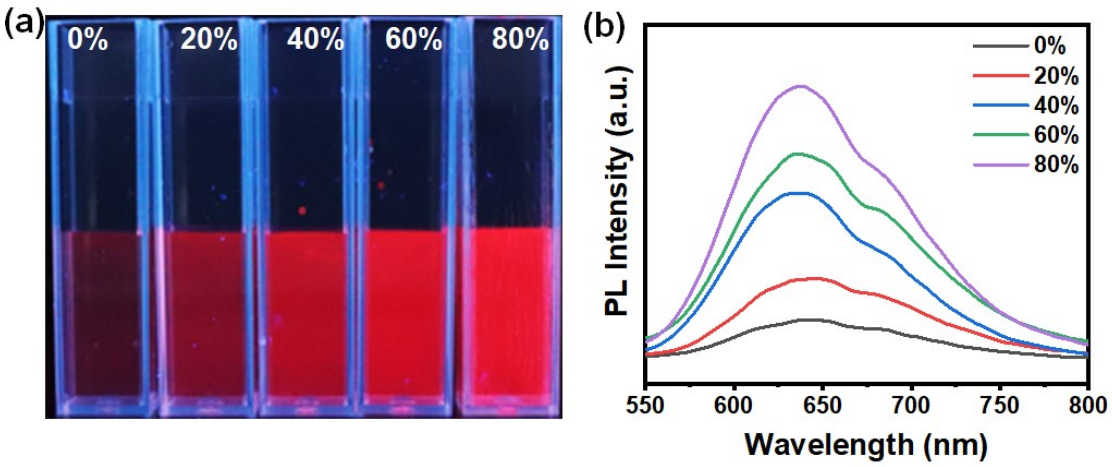

Figure S3. (a) Digital photos of AIE-typed $Ag_{28}Au_1$ NCs in mixed solvents of methanol and water with increasing methanol concentration. (b) The PL spectra of AIE-typed $Ag_{28}Au_1$ NCs in mixed solvents with increasing methanol concentration.

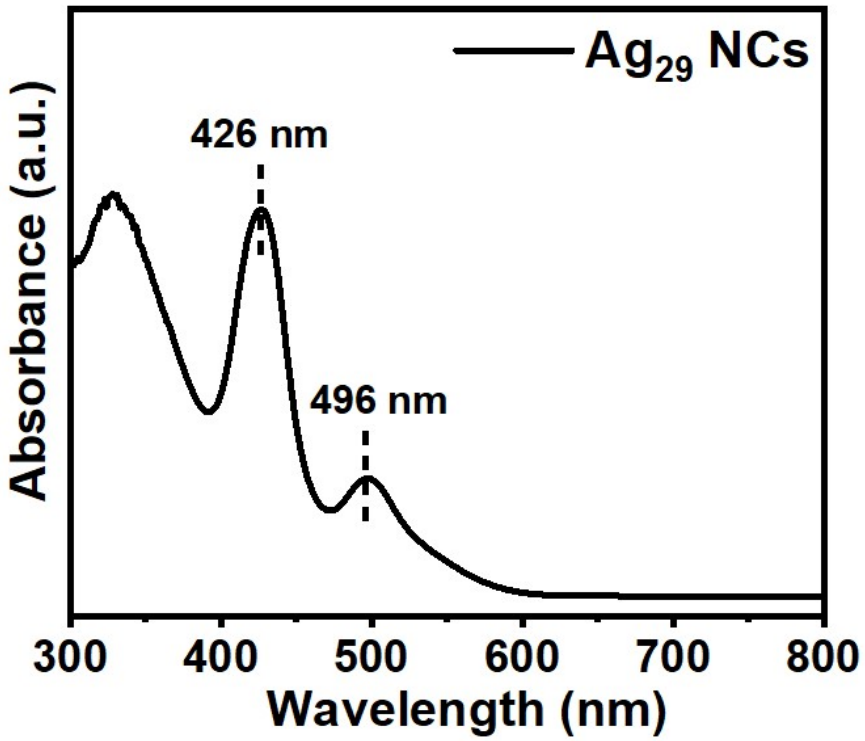

Figure S4. UV-visible absorption spectrum of Ag_{29} NCs.

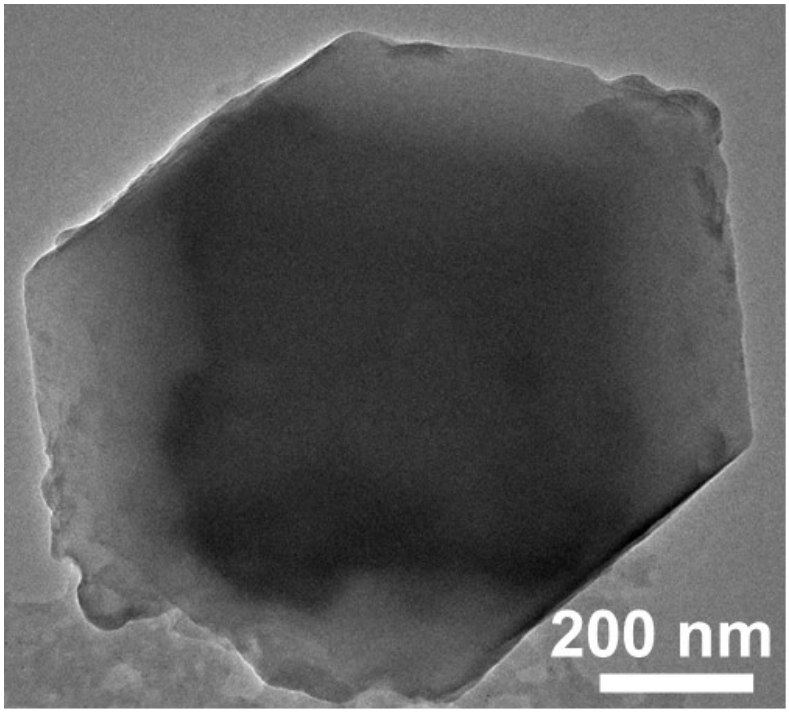

Figure S5. TEM image of the pristine ZIF-8.

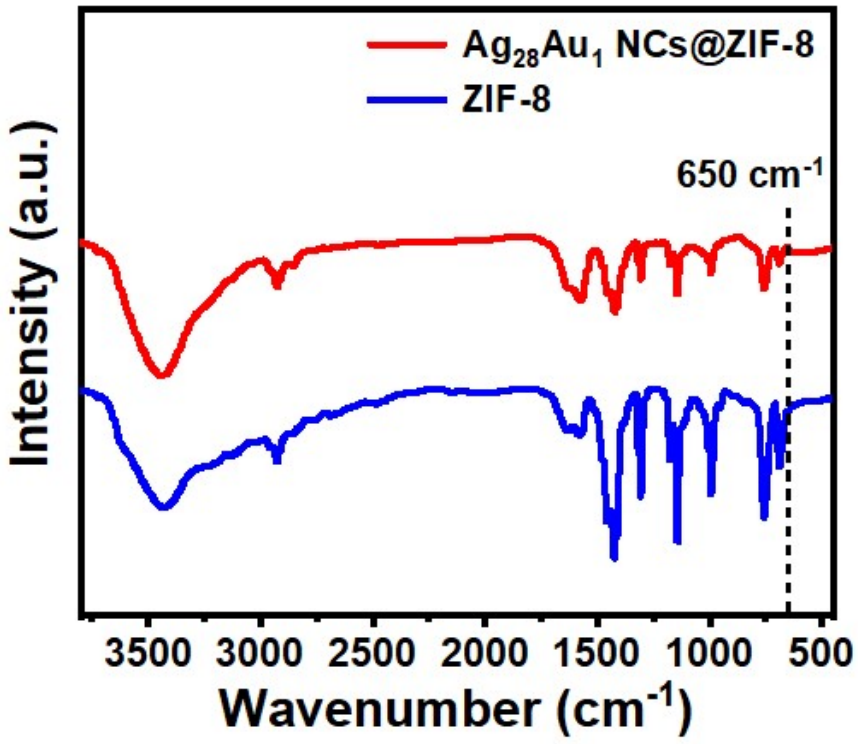

Figure S6. FTIR spectra of $Ag_{28}Au_1$ NCs@ZIF-8 and ZIF-8.

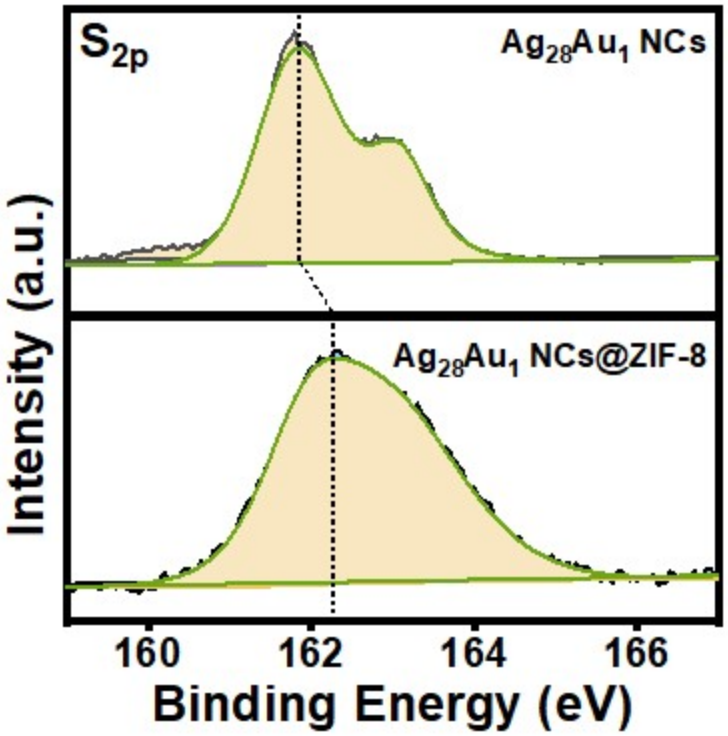

Figure S7. High-resolution XPS of S_{2p} in the $Ag_{28}Au_1$ NCs@ZIF-8 and $Ag_{28}Au_1$ NCs.

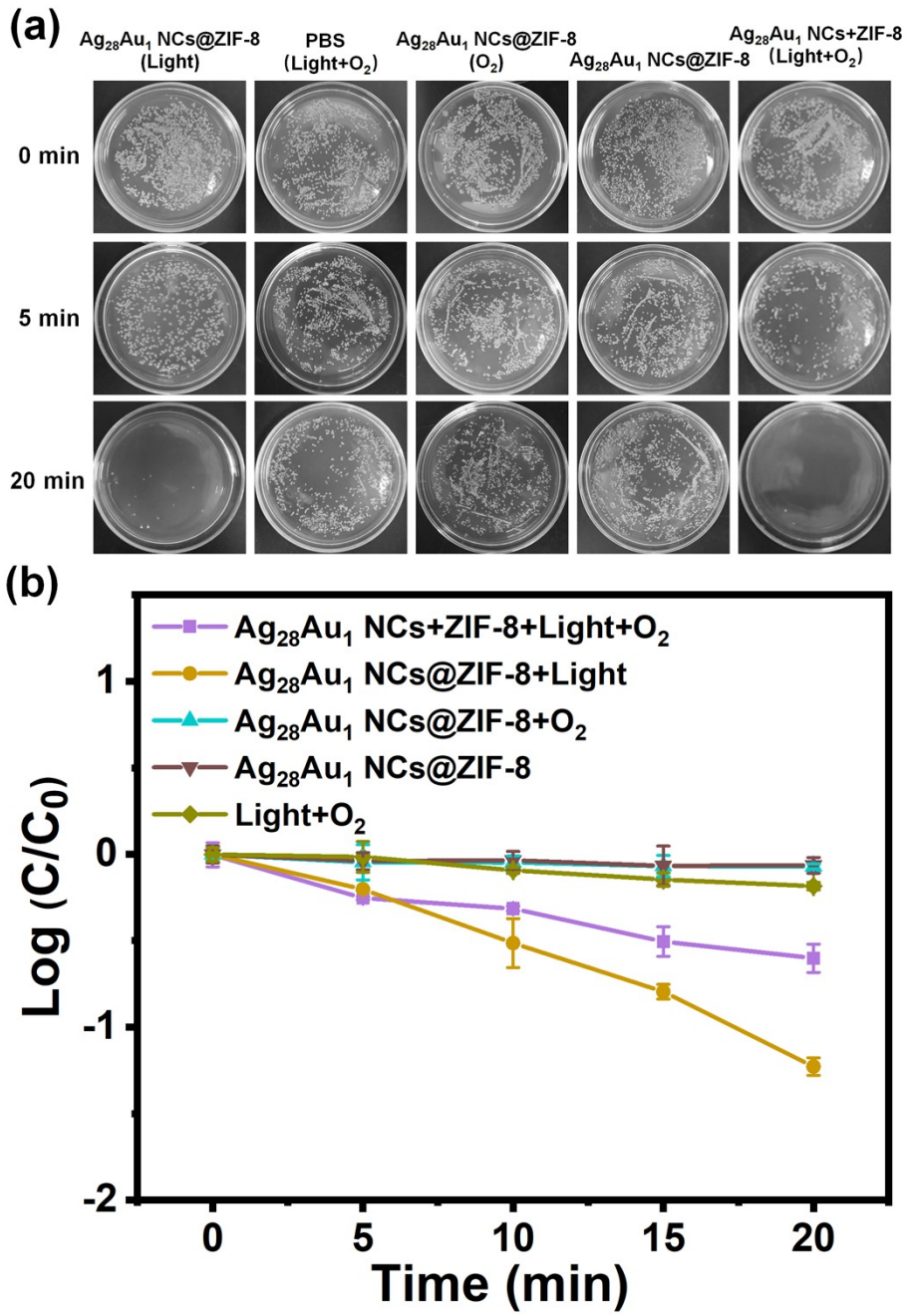

Figure S8. (a) Bacterial colony growth of *E. coli* treated with various samples under different conditions. (b) Bactericidal activity of various samples against *E. coli* under different conditions.

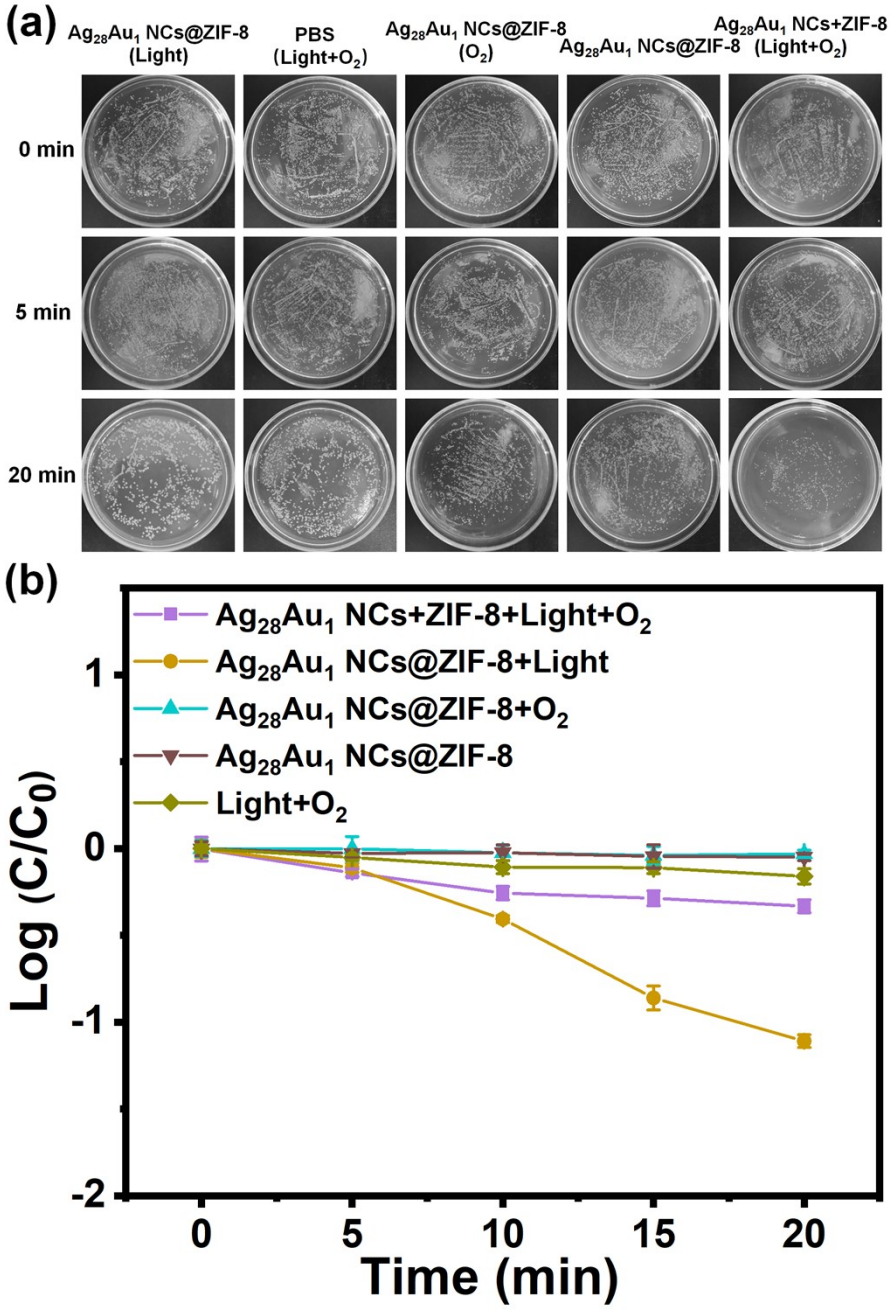

Figure S9. (a) Bacterial colony growth of *S. aureus* treated with various samples under different conditions. (b) Bactericidal activity of various samples against *S. aureus* under different conditions.

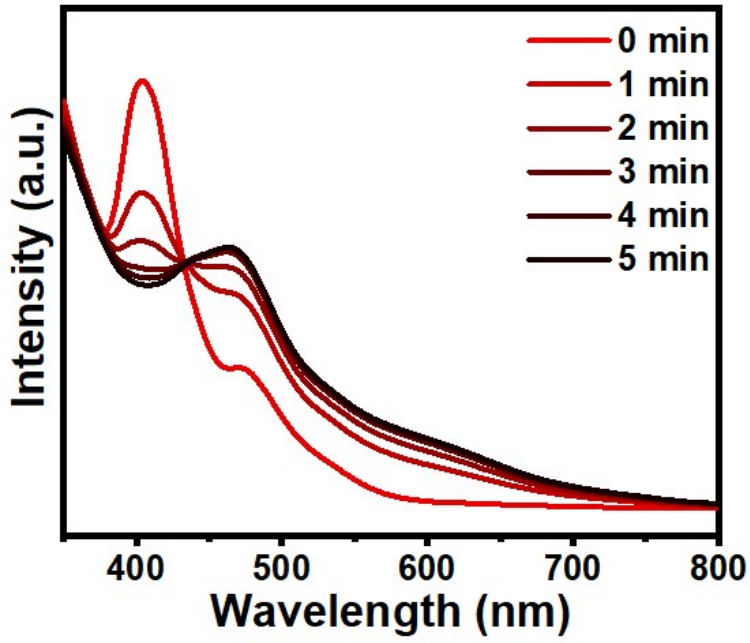

Figure S10. The UV-visible absorption spectra of the pristine $Ag_{28}Au_1$ NCs under visible light irradiation within 5 min.

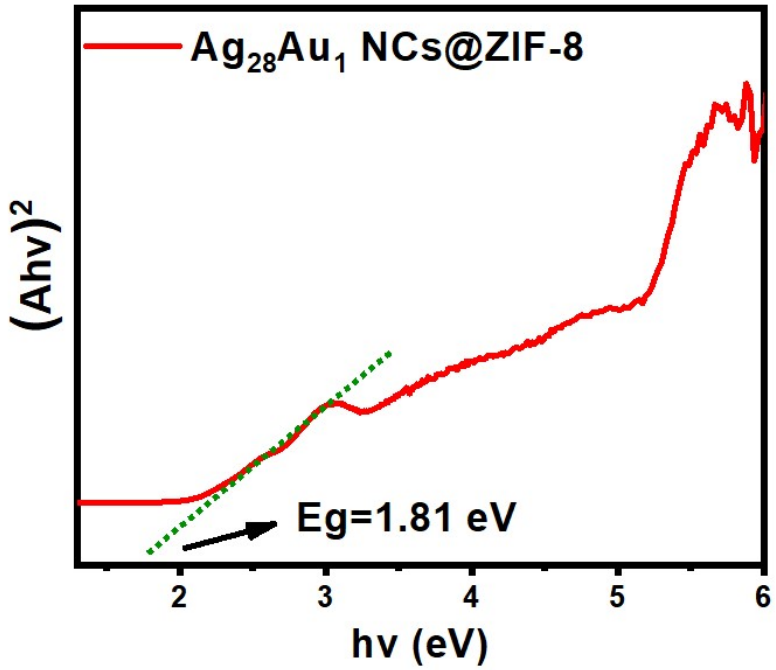

Figure S11. The plot of $(Ahv)^2$ versus photon energy of $Ag_{28}Au_1$ NCs@ZIF-8.

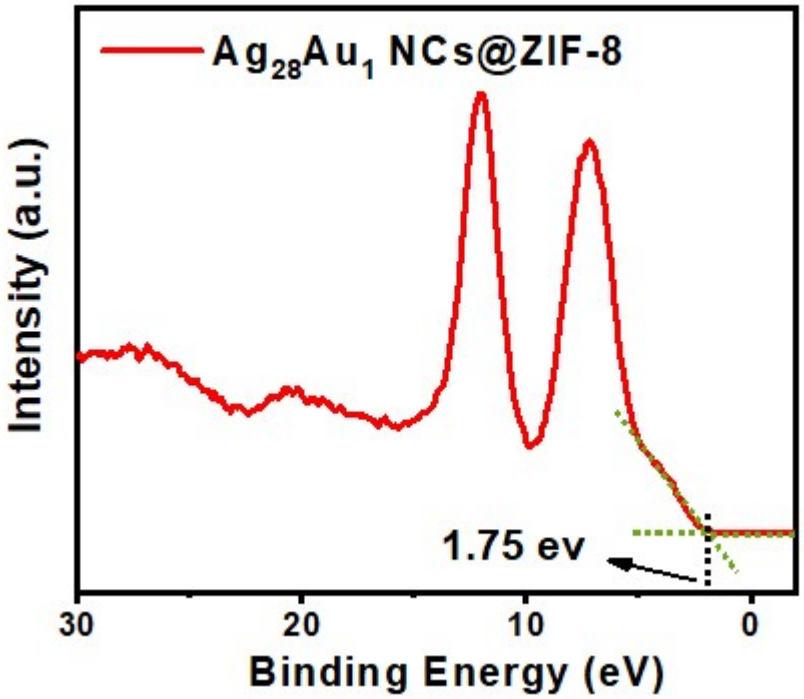

Figure S12. The VB-XPS of $Ag_{28}Au_1$ NCs@ZIF-8.

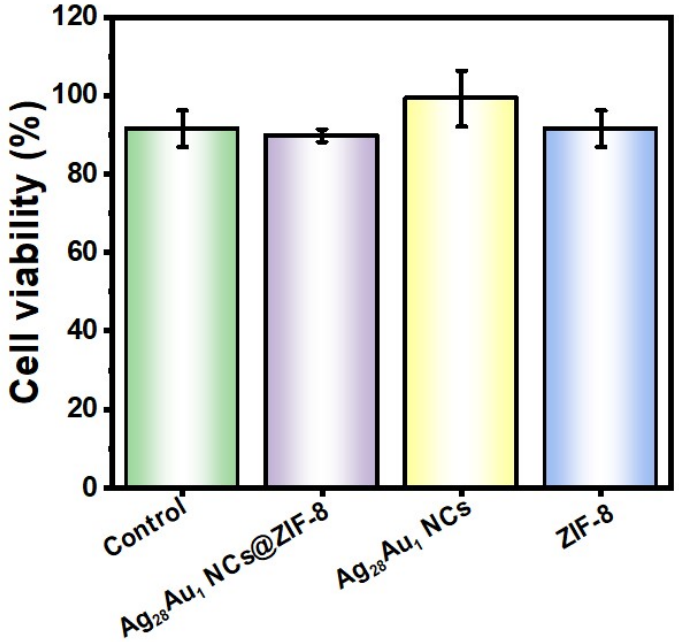

Figure S13. The cell viability incubated with carbomer (control) and various photodynamic antibacterial agents (dispersed in carbomer) incubated for 24 h.

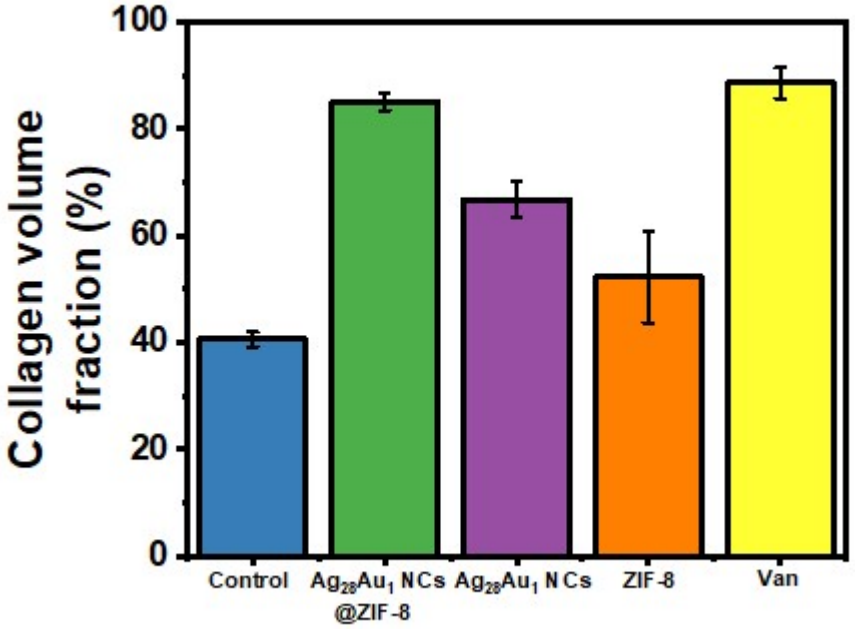

Figure S14. The collagen contents in tissue slices collected from different treatment groups on day 11.